Fermilab Proposal 600

Scientific Spokesman: J. W. Cronin
Enrico Fermi Institute
University of Chicago
Chicago, Illinois 60637

PROPOSAL TO STUDY NEUTRINO-ELECTRON AND ANTINEUTRINO-ELECTRON SCATTERING

James W. Cronin and Morris L. Swartz

Enrico Fermi Institute
University of Chicago
Chicago, Illinois 60637 USA

May, 1978

INTRODUCTION

The importance of neutrino-electron elastic scattering has been well documented, and has been the subject of other proposals to Fermilab. We will not repeat these arguments in detail here.

The cross sections expected for the reaction are very small ranging from 10^{-42} E_ν to 10^{-41} E_ν cm^2. The Weinberg-Salam model makes precise predictions for these cross sections. With $\sin^2\theta_W = 0.25$, a value which is derived from neutrino-nucleon scattering, one predicts $\sigma_{\bar{\nu}\mu e^-} = \sigma_{\nu\mu e^-} = 1.4 \times 10^{-41}$ cm^2. Measurements at the CERN PS by the Gargamelle and Aachen-Padua[1] groups are in agreement with these values. A recent result from Gargamelle at the SPS finds $\sigma_{\nu\mu e^-} \sim 7 \times 10^{-41}$ E_ν cm^2 based on ten events.[2] This unexpected result stresses the need for further investigation of these purely leptonic processes.

While a heavy liquid or Ne-H_2 bubble chamber is the ideal device to investigate ν-e scattering, only about ten tons of target mass is available. At Fermilab with the broad band beam[3] one can expect only 0.32 events/ton for 10^{18} incident protons for the Weinberg-Salam cross section. Here we propose a detector with 500 tons of fiducial volume which is dedicated to a measurement of $\sigma_{\nu e}$ and $\sigma_{\bar{\nu}e}$. This will yield ~100 events/10^{18} after cuts and background subtraction.

The detector is a tank containing distilled water. It is 4 x 4 x 60 meters and is viewed by 2000 photomultipliers. The neutrino electron scatters are characterized by the appearance in the detecting medium of an isolated electron at very small angles to the beam. The angle of the electron is given by:

$$\theta_e = \sqrt{\frac{2m_e}{E_e}(1-y)} \qquad \text{where } y = \frac{E_e}{E_\nu}$$

and is typically a few mrad at Fermilab energies, and is comparable to the angular resolution of most proposed detectors including this one.

As in other proposals we plan to use this high degree of correlation with the initial beam direction as part of the signature of the event. We use the Cerenkov radiation of the electron shower to convey the angular information of the electron shower to the walls of the detector. The detectors at the walls of the tank have a response which is sensitive to the angle of a single collimated source of radiation, such as an electron shower or muon, and can reject with a factor ~100 hadron showers which are comprised of several collimated sources of radiation. To be successful the apparatus must reject by a factor 10^4 the larger rate of neutrino-nucleon interactions.

In subsequent sections we will describe (1) the basic idea of the detector, (2) the actual proposed detector and our investigations of its energy and angular resolution, (3) the rejection of backgrounds, and (4) operational characteristics and required ancillary apparatus.

PRINCIPLE OF THE DETECTOR

Imagine a box of liquid with a relativistic muon passing through producing Cerenkov radiation. The Cerenkov light is viewed by two windows parallel to the radiation as shown in Fig. 1a. If the muon trajectory is exactly parallel to the windows, then the Cerenkov light for a fully relativistic particle will be exactly totally internally reflected at the window-air interface, and no light

will emerge. If the muon is directed towards one window, as in Fig. 1b, light will emerge from the window towards which the particle is directed. One has a device then that can measure the sign of the direction of a single particle.

The directional information can be improved if the windows are tilted (biased) with respect to the axis of the detector (Fig. 1c). Then even a parallel track will produce light in both windows. If the windows are tilted at an angle of 25 mrad one would expect a response as shown in Fig. 1d. Here one can get a quantitative measure of the projected angle of passage of the particle in the range of ±25 mrad.

In order to test these ideas and some of the properties of the optical systems that we propose to use, we have built a device similar to Fig. 1c and have tested it using cosmic ray muons. These tests are described in an appendix to this proposal.

PROPOSED DETECTOR

The detector we have studied by computer simulation consists of a box containing 2000 windows. An isometric drawing is shown in Fig. 2. On each face there are fifty rows of windows, each row containing ten windows transverse to the beam direction. Each window is 35 cm wide and 100 cm long. The rows are spaced 120 cm apart so fifty rows give a detector of sixty meters length. The fiducial volume of the detector is considered to be 3m x 3m x 55 meters giving 500 metric tons if the filling is water as considered here.

With this detector we use the principle described in the previous section and apply it to the case of an electron shower. Figure 3a shows the projected angular distribution of 0.1 rl long elements of a 25 GeV electron shower with respect to a plane parallel to the shower axis. Superimposed on the distribution is the transmission coefficient of the window, biased at 25 mrad, calculated from the Fresnel equations. The polarization vector of the Cerenkov light lies in the plane of the radiating element and the light ray. For incidence on a window perpendicular to this plane, the light transmission rises very rapidly from total internal reflection (65% transmission at 10 mrad beyond the cutoff).

As the shower axis tilts towards one surface the integrated light through the surface increases, while that through the opposite surface decreases. The range of projected angle, where there is a quantitative measure of the projected shower angle, is governed by the width of the angular distribution of shower elements and is ~±75 mrad. We have found that if light is accepted over too broad a range in angle of the shower elements, the fluctuations of the wide angle components of the shower decrease the possible angular resolution.

To effectively "truncate" the averaging of the angles of the elements of the shower we have chosen a very specific optical system which is shown in Fig. 3b. This system has the property that it mainly accepts light from a radiating element whose projected angle with respect to a face lies between -25 mrad and +100 mrad. For an element lying in a plane parallel to the face, light is accepted for angles ±200 mrad with respect to the axis of the apparatus.

While, in principle, the difference of the light collected between two faces is a measure of the projected angle, two effects must be considered in designing an algorithm to reconstruct the angle. If the shower is produced

off the central axis of the tank, there will be a difference in light arriving due to absorption in the water. Secondly, it is important to consider not only the light transmitted through the windows, but also the fate of photons which reflect and are detected in subsequent windows downstream.

In order to correct for these effects it is necessary to know the position of the shower in the tank. Figure 4 shows the amount of light received at the row of windows at shower maximum for an event.

The center of gravity of each distribution gives the projection of the shower on that surface with a standard deviation of 2 cm.

We have calculated the resolution of the detector for electron showers with a simple algorithm:

$$\theta_{\text{projected}} = \alpha \frac{U-D}{U+D},$$

where U and D are respectively the number of photoelectrons detected by a given face and its opposite. In the calculation we assume an effective absorption length of 13 meters in water of the light in the frequency spectrum corresponding to an S11 photo-cathode response. We assume that if all the Cerenkov light emitted by a 3.7 cm long electron element were to strike a photo-cathode, we would detect 80 photoelectrons. This corresponds to a figure of merit $N_c = 50 \sin^2\theta_c$ photoelectrons/cm. As noted in the appendix, this may be optimistic. The qualities U and D have small corrections (~5%) which are position dependent. We assume the energy is proportional to the amount of light. In Table I we give the energy and angular resolutions for electron showers which we can expect for the apparatus for electrons within 30 mrad of the axis.

TABLE I

Electron Energy (GeV)	$\sigma_{\theta_{projected}}$ (mrad)	$\sigma_{E/E}$ (%)	Mean number of photoelectrons	σ_{θ_p} (1/2 pe)
5	7.0	5.7	2500	7.2
15	5.0	4.6	7900	5.2
25	4.0	3.2	13200	4.2
35	3.5	3.0	18500	3.6

These resolutions depend on the fluctuations in the showers and perhaps position in the tank, but do not depend on the number of photoelectrons as indicated by the fifth column. No light is recorded if it produces less than five photoelectrons in a given tube.

Figure 5 shows the correlation of the quantity U-D/U+D with angle for 25 GeV showers. The two quantities are related by U-D/U+D = 12 $\theta_{projected}$.

REJECTION OF BACKGROUNDS

Rejection of unwanted events is the heart of the experimental problem. There are three main classes of events which can cause difficulty. These are

1. Inverse β decay from the ν_e contamination in the beam.
2. Neutral current events and charged current events where the muon is not identified.
3. Deep inelastic scattering of the ν_e background in the beam with small x and small y.

The two means we have to reject these backgrounds are:

(a) Separation of electron showers from hadron showers,

(b) Separation of the ν_e scatters by distribution in the variable $E_e\theta^2$.

We assume that the backgrounds will be characterized by angular distributions that are broad compared to those expected for ν-e scattering and that an appropriate plot such as a plot of events versus $E_e\theta^2$ will show a peak for $E_e\theta^2 < 2\ m_e$ above a smooth background.

This is the situation for the inverse β-decay background. Figure 6 shows a calculation of what one expects for the signal on top of the inverse β decay background. The calculations were made assuming that $\sigma_E/E = 17/\sqrt{E_e}$ % and $\sigma_{\theta_p} = 20/\sqrt{E_e}$ mrad. The ν_e contamination was assumed to be 1% of the ν_μ. The data are plotted against the variable $E_e\theta^2$ which should range from 0 to 2 m_e with perfect resolution, and are smeared by the resolution. It is interesting to note that the spatial angular resolution $\sigma_{\theta_s} = 28/\sqrt{E_e}$ is always matched to the available angular range $\theta = \sqrt{2m_e/E_e} = 33/\sqrt{E_e}$.

A far more serious background comes from neutral current interactions. The cross section is ~0.2 $E_\nu \times 10^{-38}$ and can occur on both neutrons and protons. The relative cross sections are thus effectively:

$$\sigma_{NC}/\sigma_{\nu e} \sim 0.4 \times 10^{-38}/0.14 \times 10^{-41} \simeq 2.8 \times 10^3.$$

We have begun studies of the hadron rejection in our apparatus. What we report here is preliminary and will be updated in a subsequent report.

Andreas Van Ginneken of Fermilab has provided us with a calculation of 1000 hadron showers in a format suitable for the generation of Cerenkov radiation by the charged, and neutral pions and protons in the liquid. The hadronic showers were selected with an energy spectrum which would result from a flat y distribution.

The response of our detector to hadronic showers is qualitatively different from electron showers. First, on the average, the fraction of energy of the hadron showers as seen in Cerenkov light is considerably less than electron showers. This is principally because the directions of many of the components of the shower are at angles beyond the angular sensitivity of the detector. On average a hadron shower produces only about 60% of the Cerenkov light of an electron shower of the same energy. There are large fluctuations, and many hadrons tend to pile up at low energy. Figure 7 shows the input hadron energy spectrum and the apparent hadron energy spectrum as viewed by the detector. For the purpose of further discussion, we assume that we cut the data for energies below 5 GeV. This cut will eliminate 15% of ν-e events for a flat y distribution, and will eliminate 35% of the events for a $(1-y)^2$ distribution, and a negligible amount for a y^2 distribution.

A second discriminator of the hadron shower events is the fact that the light appearing on the four faces has a significant component coming from different sources. This is in specific contrast to an electron shower, which on the scale of resolution of the detector is a single object. For an electron shower one can follow the projection of its path on each face by following the

centroids of the light patterns on each row. These points should be on a straight line and have, within errors, the same direction on both faces. Furthermore, the projected position on opposite faces of the detector should be identical.

Figures 8a and 8b illustrate these points. In Fig. 8a, we plot the mean square deviation of the centers of gravity of light in successive rows of detectors from the best fit straight line. One can observe a marked difference between electron showers and hadron showers. The fits to a straight line are made only for the first four rows on each face which receives greater than five photoelectrons. Figure 8b shows the distribution of the differences of the centers of gravity of light on opposite faces. If the light on opposite faces is coming from separate radiating particles, then the center of gravity of the light on opposite faces can differ significantly. The combined cuts on the two variables described above plus the requirement that the energy be larger than 5 GeV reduces the hadrons with respect to electron showers by approximately a factor of 100.

A second rejection factor of 100 can be obtained by examination of the apparent angular distribution of the remaining hadrons determined by integrated light balance on the faces. These are spread over a polar angle of ~50 mrads. Since the angles of interest are of the order of 5 mrads for the collimated electron showers, an additional factor of ~100 is obtained.

These conclusions about the rejection of the hadron events are based on only a brief period of study of the response of the apparatus to hadrons.

By more careful study of the problem and modifications of the optics of the light collections we hope to further improve the hadron rejection so as to increase the safety margin.

The background source 3 is also a very serious one. Here we consider inelastic scattering of the contamination ν_e in the beam producing very little hadronic energy. For ν_e-nucleon scattering the quantity $E_e\theta^2$ is given by $2\ m_p xy$. The part of the deep inelastic distribution which is potentially troublesome is the region for which $xy \sim m_e/mp$. Figure 9 shows the distribution in $E\theta^2$ of ν_e-nucleon scattering in the region of $E\theta^2 = 1$ MeV. To make these calculations we assumed a distribution which was flat in y and had a dependence $(1-x)^3$ in the variable $x = Q^2/2m_p\nu$. We assumed, as above, that the ν_e contamination in the beam was 1%.

This background can be reduced further by the ability to detect a hadron shower in coincidence with the electron shower. This we can probably do for $y \geq 0.3$. In this case the background is reduced by a factor ~2 which gives a signal to noise of better than 4/1.

In conclusion it appears that the technique proposed can detect neutrino electron scatters with a background of ~30%. The signal of interest should show up as a peak at small values of $E_e\theta^2$. The background under the peak is smooth and its level can be obtained from the data itself.

MEASUREMENTS AND YIELDS

Over the course of 18 months one can hope to accumulate ~10^{19} protons on the neutrino target with the broad band beam. After cuts, this should yield ~500 $\nu_\mu e^-$ events and 250 $\bar{\nu}_\mu e^-$ events assuming $\sigma_\nu = \sigma_{\bar{\nu}} = 1.4 \times 10^{-42}$ E_ν cm^2. In addition to the total cross sections we can also measure the energy spectrum of the events, and obtain information about the y distributions.

An important ingredient in the measurements will be a constant monitoring of the charged current events signaled by a penetrating muon. We expect to have a toroid magnet downstream to analyze the momentum of exiting muons. This rate and spectrum will be the standard by which the ν_e scattering cross section and spectrum will be compared. A muon is easily identified in our apparatus and its projected angle can be determined with a standard deviation of 2 mrad if its energy is greater than 10 GeV.

OTHER REMARKS

We will require occupancy in the broad band horn focused neutrino beam for at least two years. We will also require a means of directing a hadron, muon and electron beam into our apparatus for calibration.

We expect to run this apparatus in a non-triggered mode which is nearly dead time free. Each phototube will trigger a local discriminator at a level of five photoelectrons. For an RCA 8055 PM this produces a rate of ~1000 hz. This pulse will trigger the entry of a 10 mhz clock reading into a local memory and dump the charge from the PM onto a condensor with an FET switch. On the average one expects ~100 events/pulse each with an average of 100 phototubes going. This means an average of 5 events/pulse in each phototube. Thus

with the capability of storage of 16 events at each station, no data will be lost.

The data is accumulated locally, the clock pulses in a local memory. When the 1 msec neutrino pulse is ended a local ADC converts the pulse heights to digital information, then sequentially the data are read out along forty 16-bit data lines to the downstream end of the apparatus where a processor will filter out undesirable events such as obvious hadrons, too little energy deposit, etc.

MANPOWER

It is obvious that this experiment requires more manpower than the present two proponents. At Chicago we are hiring in September, 1978, a good research associate who will work full time on the experiment. A second student will join the group. We have discussed collaboration informally with two other groups who have shown interest.

The experiment is basically the replication of 2000 identical units. For a small group the understanding in complete detail of one unit is not too difficult. We would hope to find one other small group that is completely dedicated to this experiment.

ACKNOWLEDGEMENTS

Work on the design of this experiment has been a great pleasure. It is obvious that the work is not complete and many questions remain to be answered. It is our style to talk freely and openly about our ideas. Many people thus have wittingly or unwittingly contributed to this experiment. First, we should mention the many people who have thought about water as a detection medium.

Among these are Bruce Brown, Art Roberts, Larry Sulak. The ideas of Dave Cutts and collaborators in the PEP 16 proposal provided the seminal idea. At Chicago we have greatly profited from discussions with Mel Shochet. Finally we want to thank our engineer Dick Armstrong for his help on many aspects of this work including the tank test, and Andreas Van Ginneken of Fermilab for his help with the hadron showers, and Charles Baltay for his gracious hospitality and critical suggestions during our visit to Nevis.

1. H. Faissner et al., to be published; H. Reithler, Proceedings of the 1977 International Symposium on Lepton and Photon Interactions at High Energies, p. 343; J. Blietschau et al., Phys. Lett. 73B, 239 (1978).

2. We used the neutrino spectrum for the two horn beam calculated by B. Baltay.

3. P. Alibran et al., CERN Preprint CERN/EP/PHYS 78-6, 1978; also to be published in Phys. Lett.

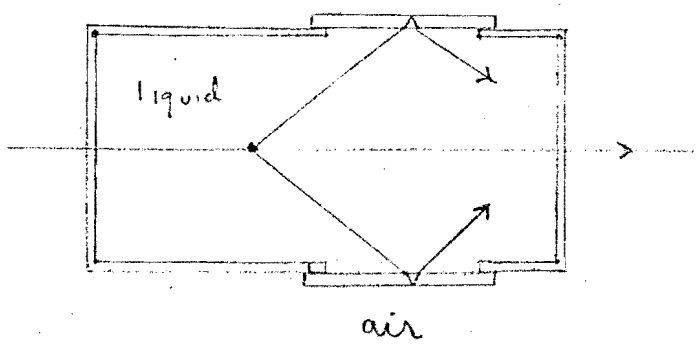

1 a

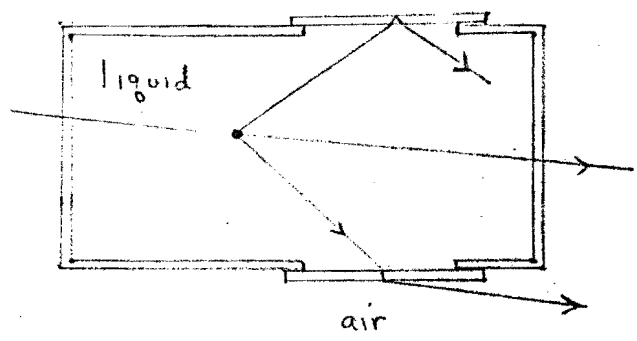

1 b

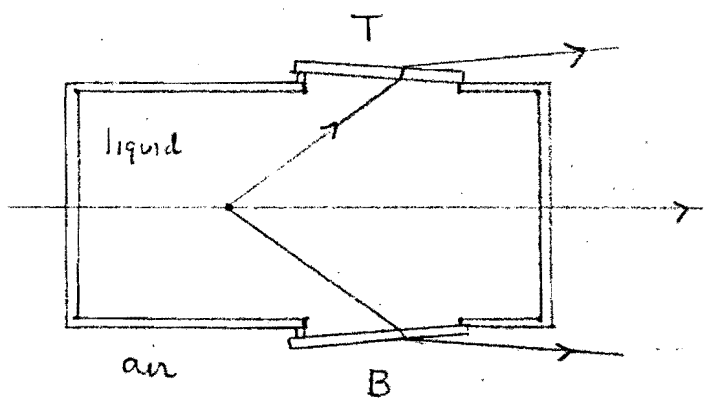

1 c

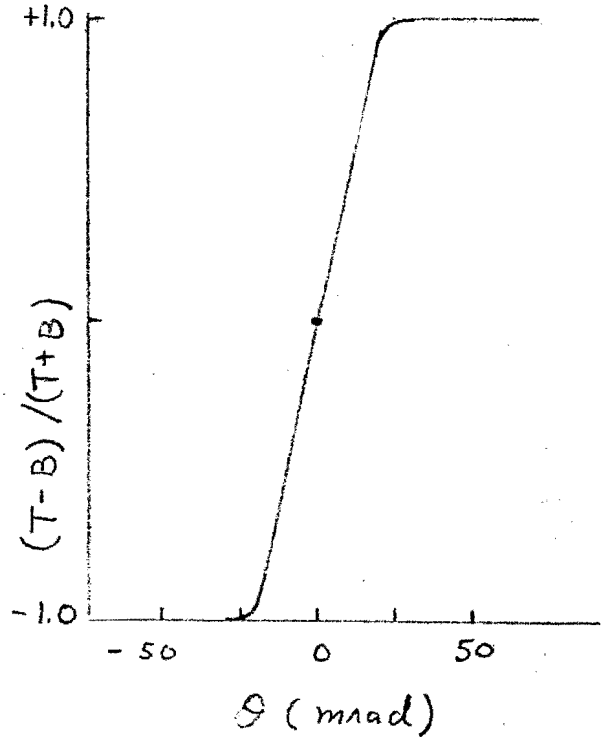

1 d

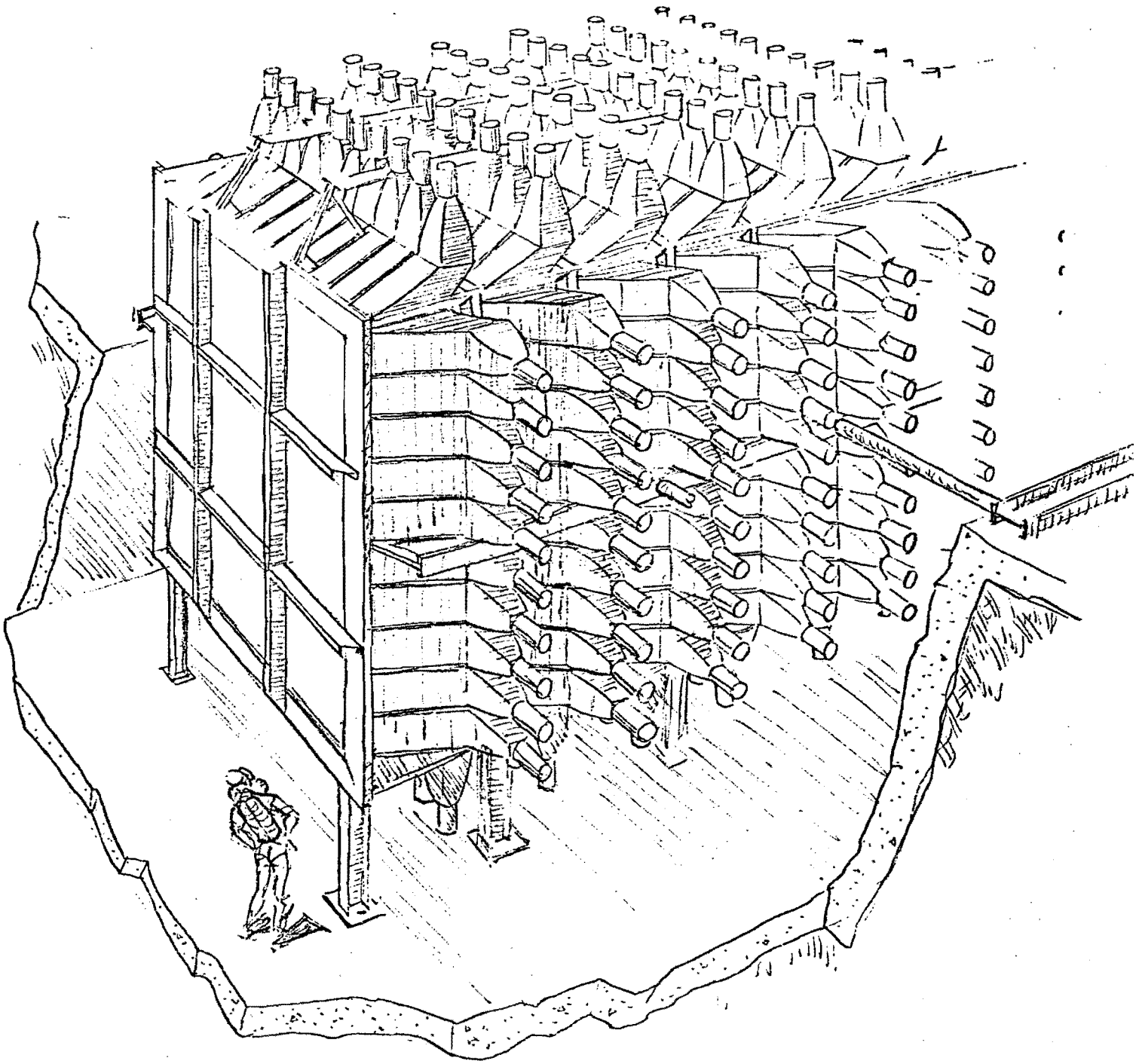

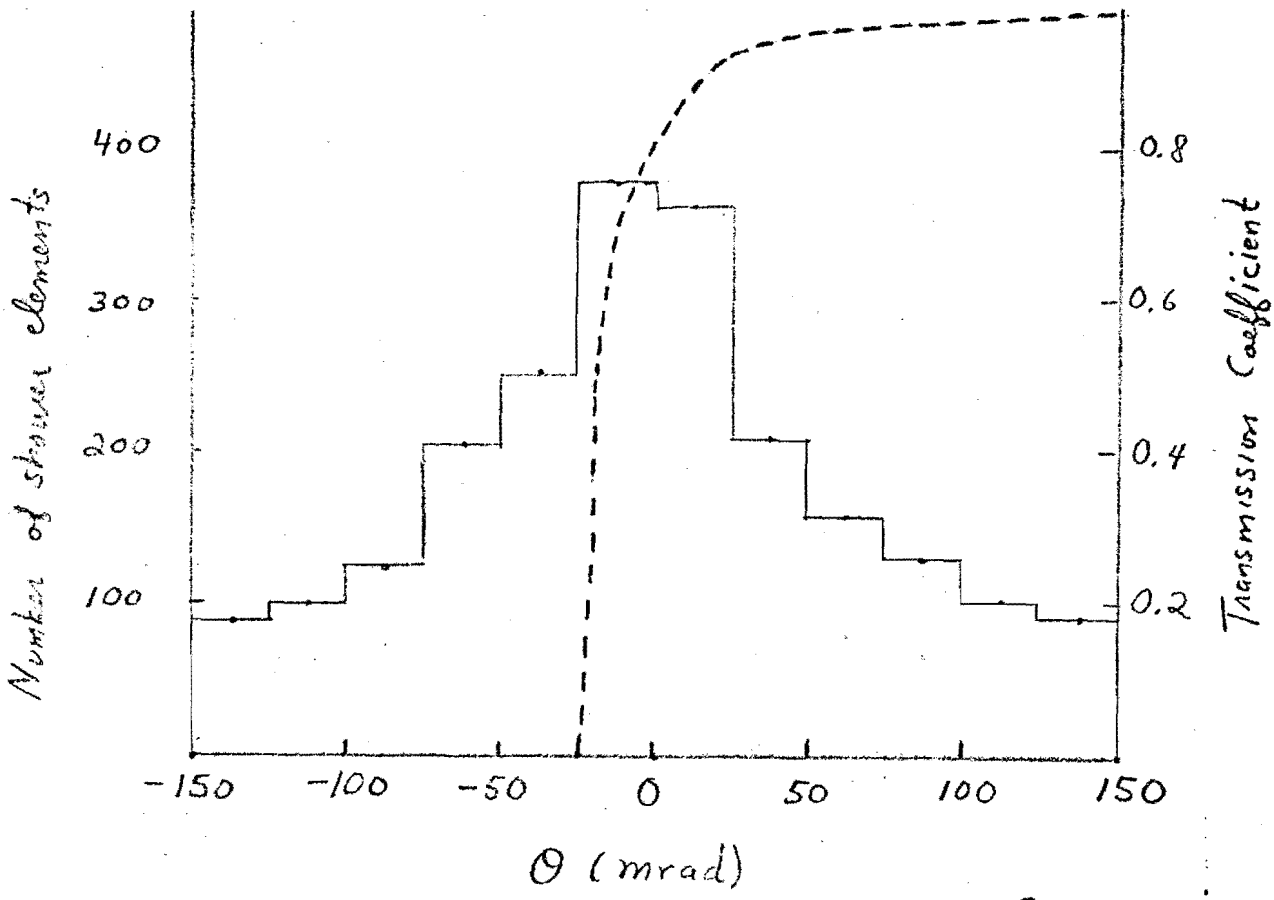
Number of shower elements
400
300
200
100
0.8
0.6
0.4
0.2
Transmission Coefficient
-150
-100
-50
0
50
100
150
θ (mrad)

3 a

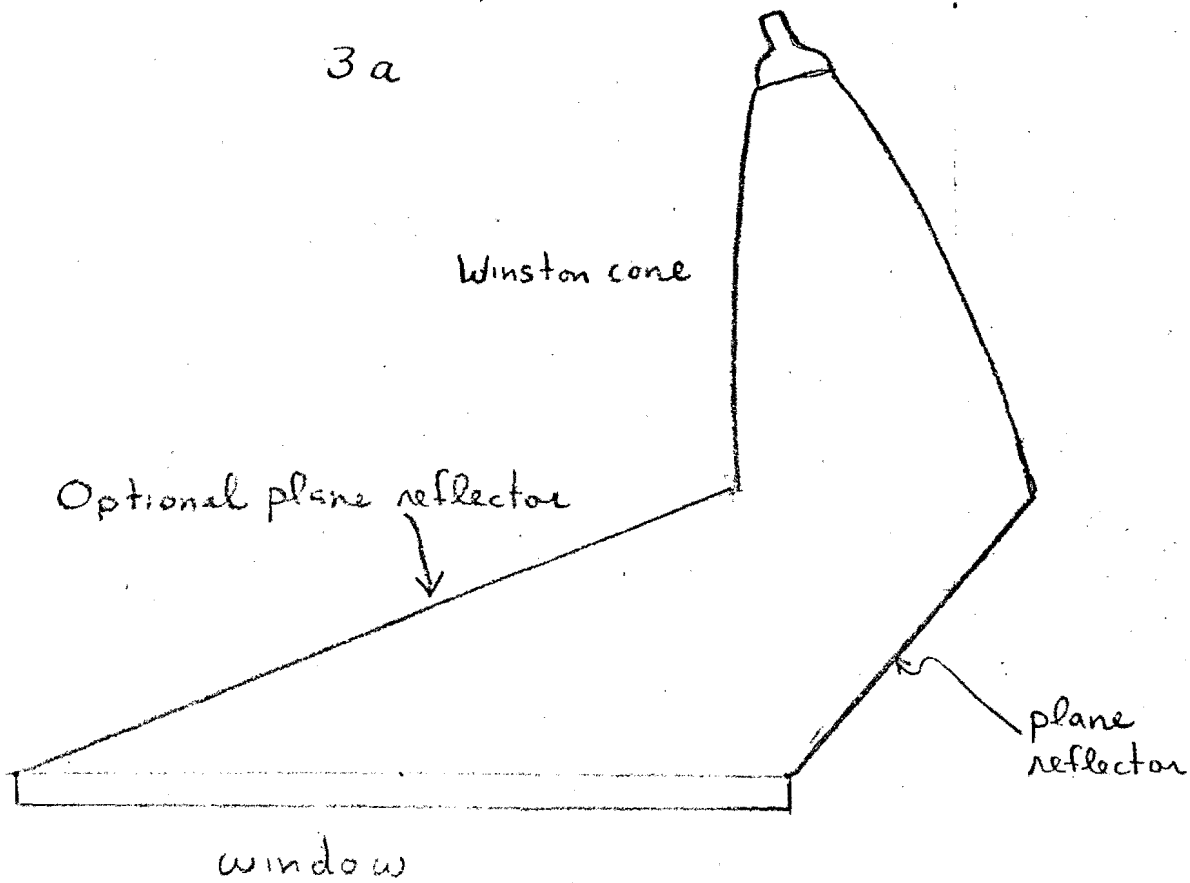
Winston cone
Optional plane reflector
plane reflector
window

3 b

Height of poker chips proportional to light received

Center of gravity of poker chips is projected position of radiating element.

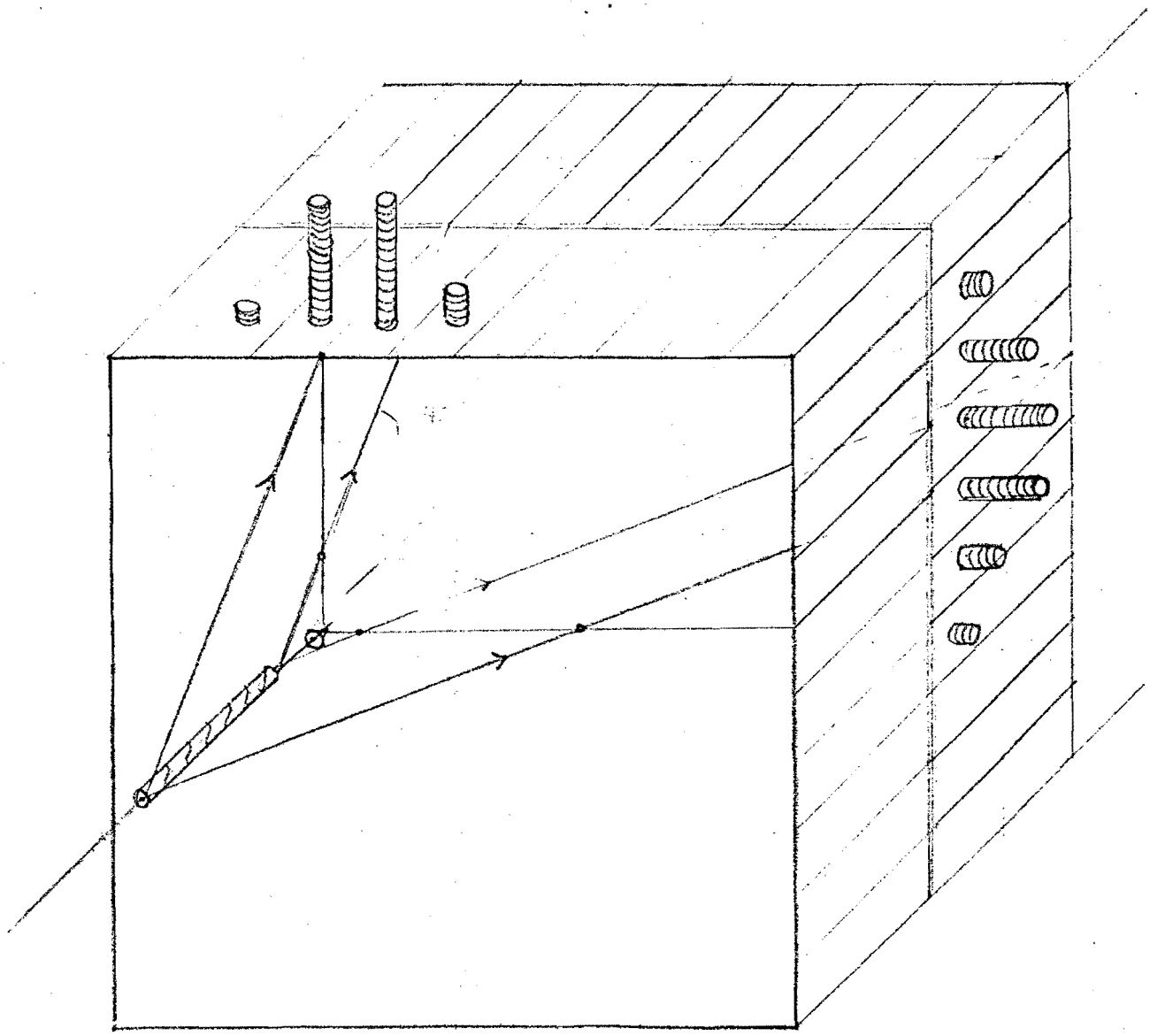

Fig 4

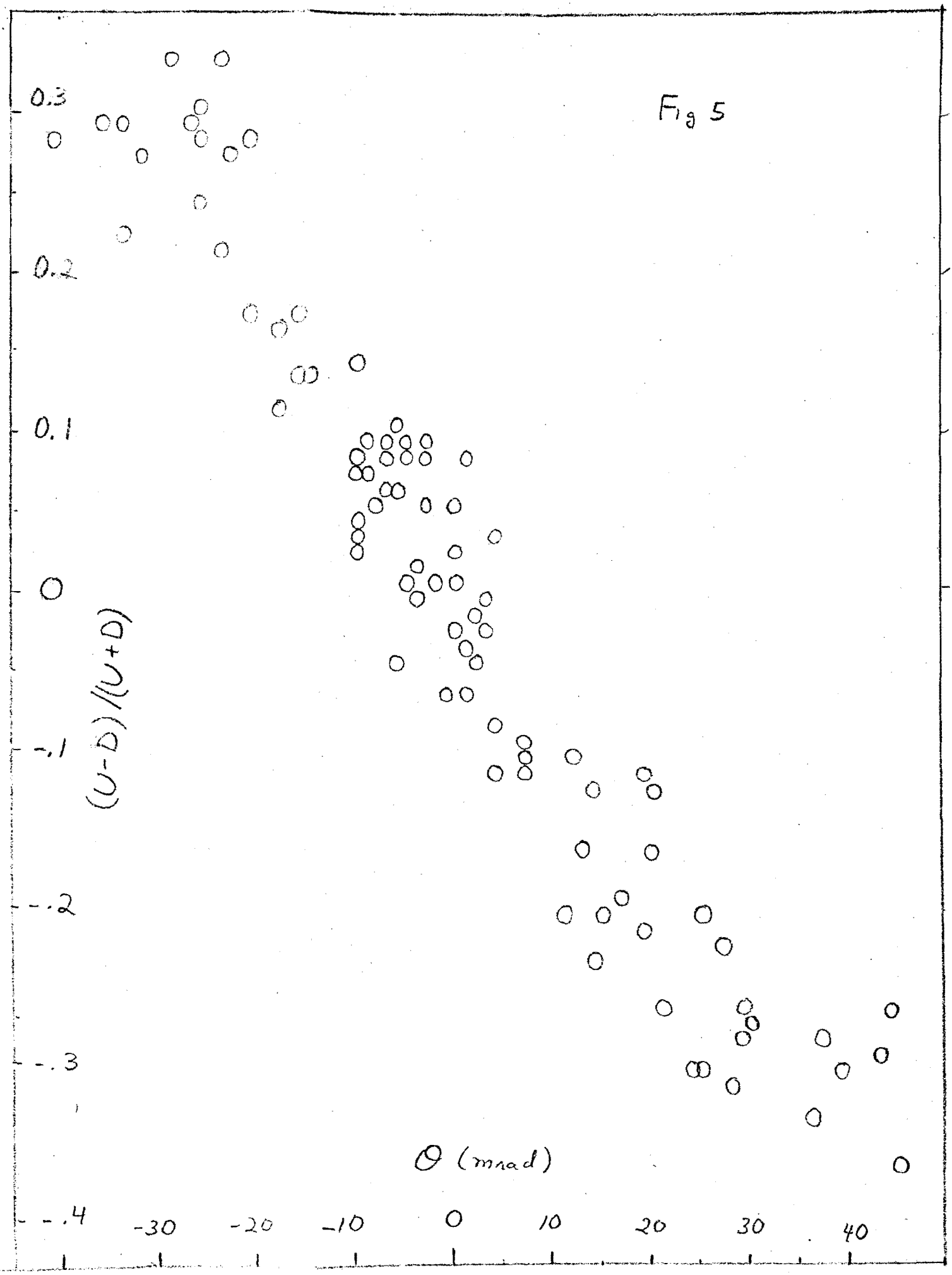
Fig 5
0.3
0.2
0.1
0
-.1
-.2
-.3
-.4
(U-D)/(U+D)
θ (mrad)
-30
-20
-10
0
10
20
30
40

Fig 6

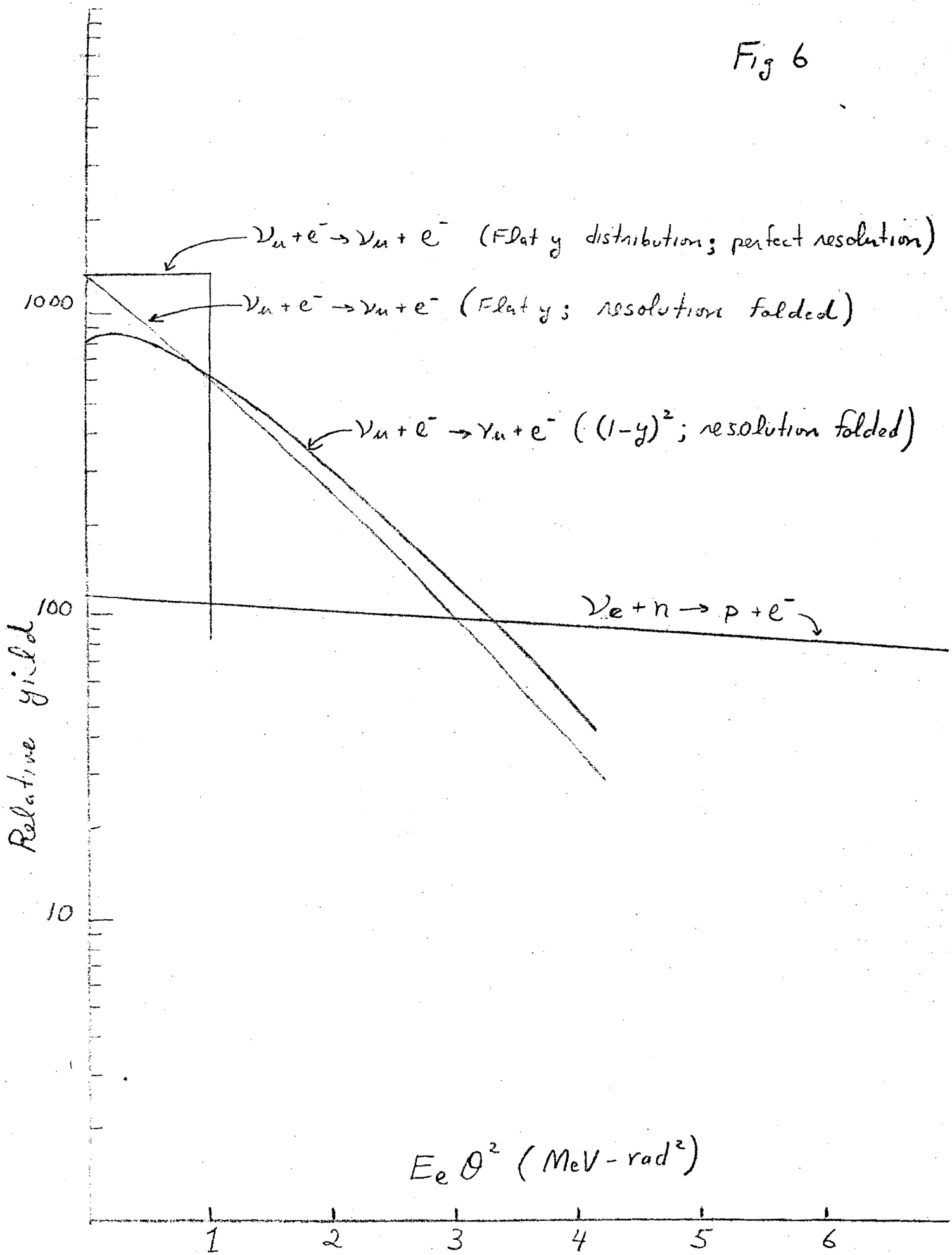
$\nu_\mu + e^- \to \nu_\mu + e^-$ (Flat y distribution; perfect resolution)
$\nu_\mu + e^- \to \nu_\mu + e^-$ (Flat y; resolution folded)
$\nu_\mu + e^- \to \nu_\mu + e^-$ ($(1-y)^2$; resolution folded)
$\nu_e + n \to p + e^-$
1000
100
10
Relative yield
$E_e \theta^2$ (MeV-rad^2)
1
2
3
4
5
6

Fig 7

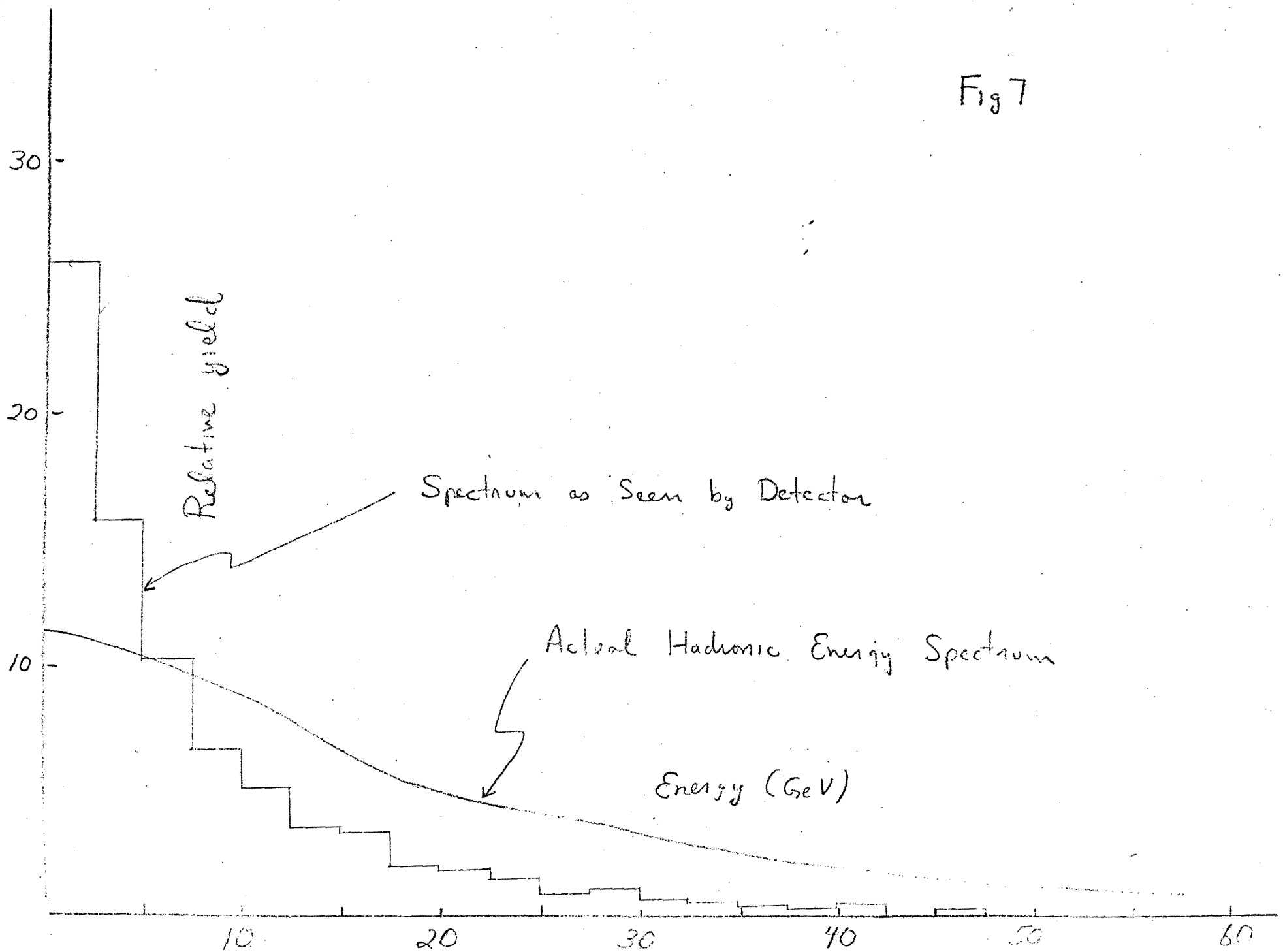
30
20
10
Relative yield
Spectrum as Seen by Detector
Actual Hadronic Energy Spectrum
Energy (GeV)
10
20
30
40
50
60

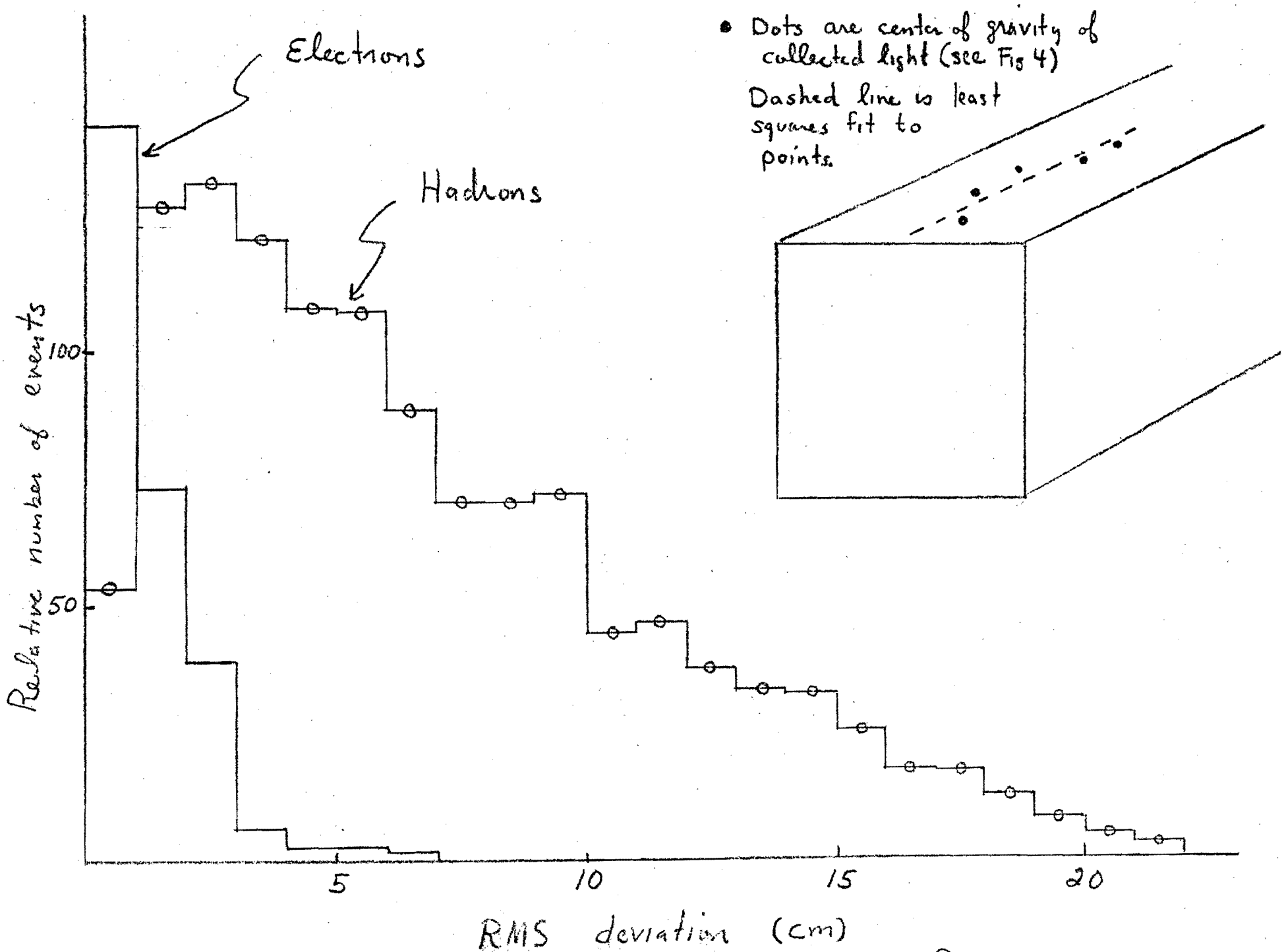
Electrons
Hadrons
• Dots are center of gravity of collected light (see Fig 4)
Dashed line is least squares fit to points.
Relative number of events
100
50
5
10
15
20
RMS deviation (cm)

Fig. 8 A

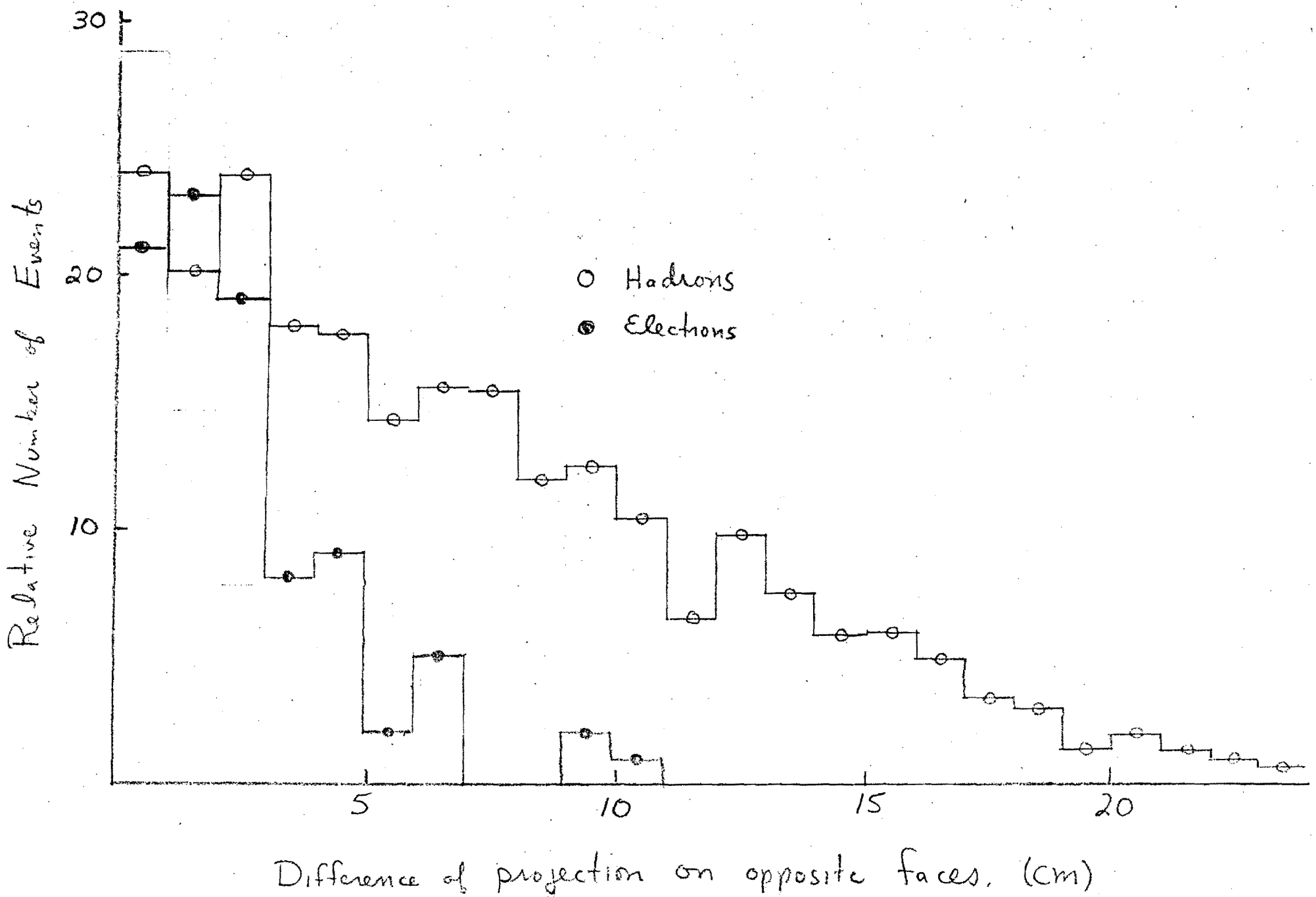
30
20
10
Relative Number of Events
Hadrons
Electrons
5
10
15
20
Difference of projection on opposite faces. (cm)

Fig 8 B

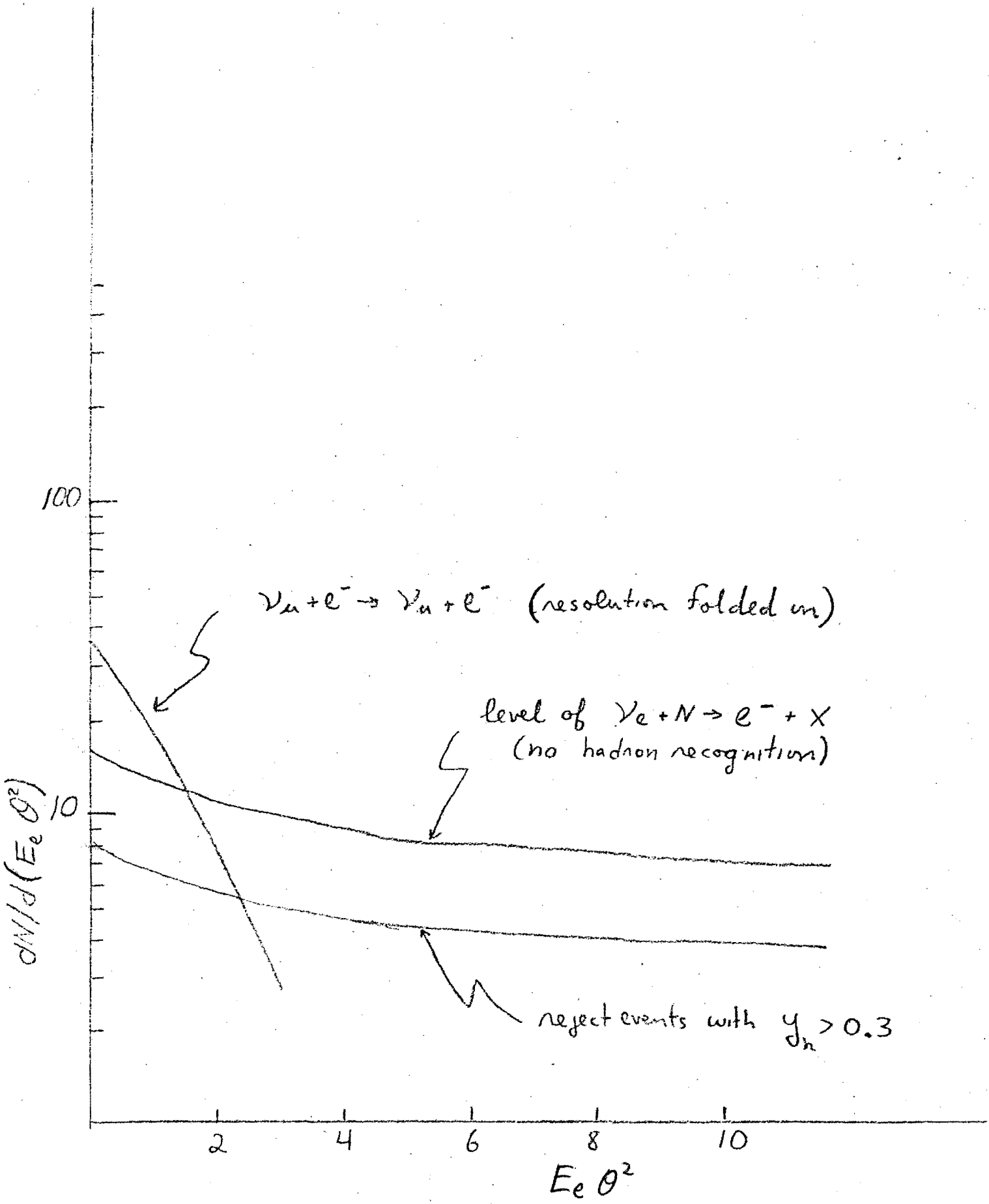
100
10
$\nu_\mu + e^- \to \nu_\mu + e^-$ (resolution folded in)
level of $\nu_e + N \to e^- + X$
(no hadron recognition)
reject events with $y_h > 0.3$
$dN/d(E_e\theta^2)$
2
4
6
8
10
$E_e\theta^2$

Fig 9

APPENDIX I

A detector similar to the one shown in Fig. 1c of the proposal was constructed and tested with cosmic ray muons. A schematic diagram of the test apparatus is shown in Fig. A1.

The detector consisted of 2.5' x 6' cylindrical steel tank filled with distilled water. Lucite windows, 40" x 14" x 1" thick were mounted, inclined at an angle of 25 mrad with respect to the tank axis, on flanges welded to opposite sides of the tank. The walls of the tank were painted black. Winston "perfect" light collectors were installed adjacent to the windows in plywood cowlings. RCA 8055 photomultiplier tubes were placed at the output of the light collectors.

The 1' x 1' counters, C1 and C2, were used to define the cosmic ray beam. Two 30 cm x 30 cm MWPC's (M1 and M2 in Fig. A1) provided a two-point track of individual muons. To reduce multiple scattering, a 1 GeV/c momentum requirement was included by installing 6" of lead and 2' of steel under chamber M2 and requiring a coincidence with counters C3 and C4.

Figures A2 and A3 are scatter plots of pulse height from the PM tubes versus projected angle of the tracks. Note that the maximum collected light occurs when the track is inclined by approximately 25 mrad toward the particular collector. Light emitting diodes mounted in the cowlings enabled calibration of the PM-ADC channels in terms of photoelectrons. The number of photoelectrons in the maxima of Figs. A2 and A3 is only about one-third the number expected from Monte-Carlo calculations. Since the water inside the detector appeared somewhat cloudy to the eye, it is likely that with

some care the number of collected photoelectrons can be significantly improved. A detailed investigation of the fate of photoelectrons is underway.

It is indicated in the text of this document that the projected angle of the track is expected to be linear in the variable

$$x = \frac{N_1 - N_2}{N_1 + N_2}$$

where N_1 is the number of photoelectrons generated by PM #1 and N_2 is the number of photoelectrons generated by PM #2.

A scatter plot of x versus projected track angle is shown for 1150 events in Fig. A4. Note that x varies from -1 to +1 as the projected angle varies from 25 to -25 mrad. A linear relationship is observed but with a resolution of approximately 6 mrad. This apparent lack of resolution is due primarily to the effect of multiple scattering on the two-point tracking.

The apparatus was simulated in a Monte-Carlo calculation and the results are shown in Fig. A5.

Figure A5 is a scatter plot of x versus projected track angle for events. In the region of projected angle from 25 to -25 mrad one observes that a linear relationship exists with a resolution of about 6 mrad. Thus, the Monte-Carlo shows good agreement with the data in this region. Fig. A4 shows that the distribution in x tends to curve toward x = 0 for projected angles > 25 mrad and <-25 mrad. This is due to PM noise in both tubes and the gradual cutoff in light transmission of the Winston light collectors as the projected track angle increases.

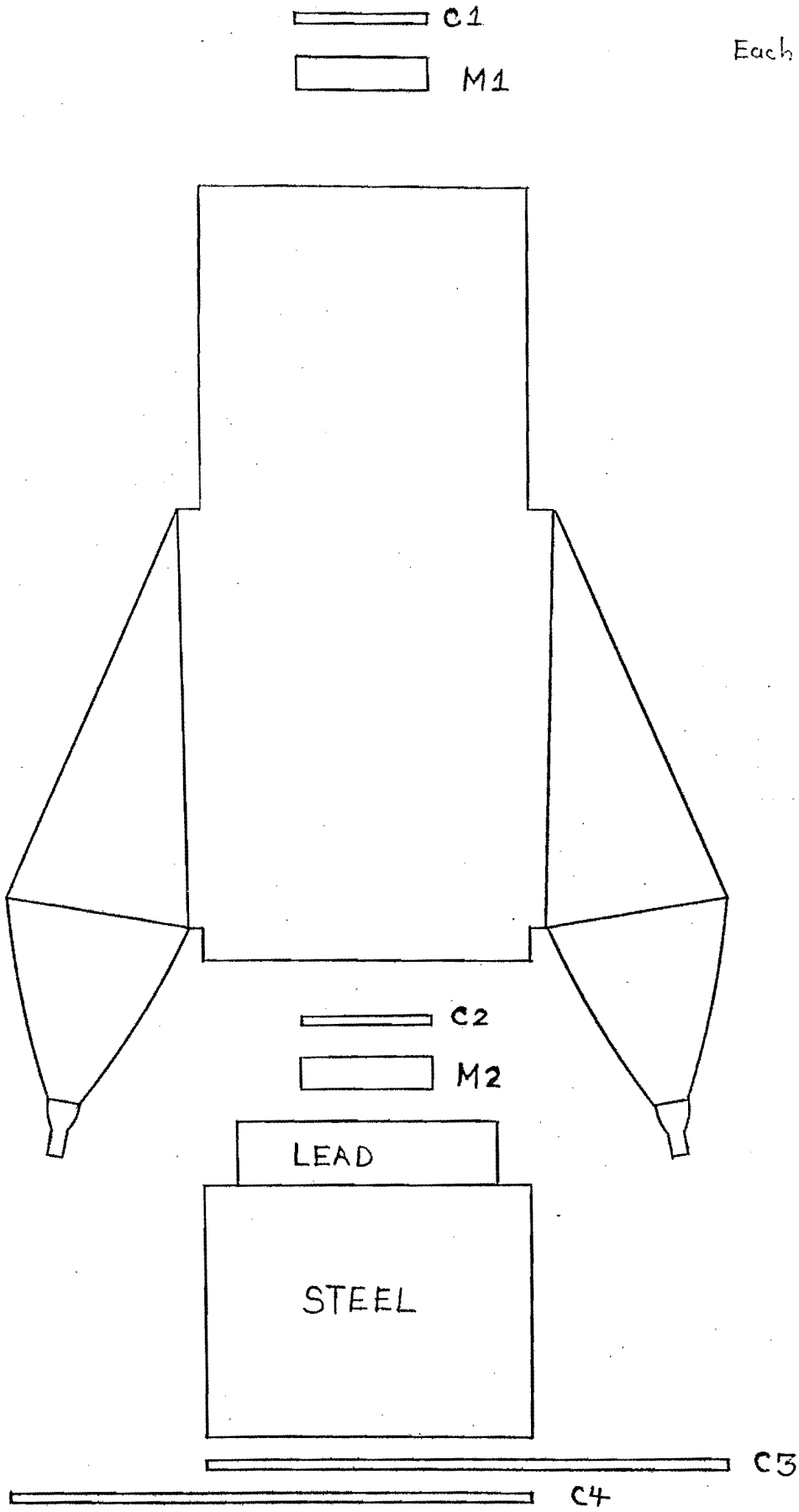

Fig. A1

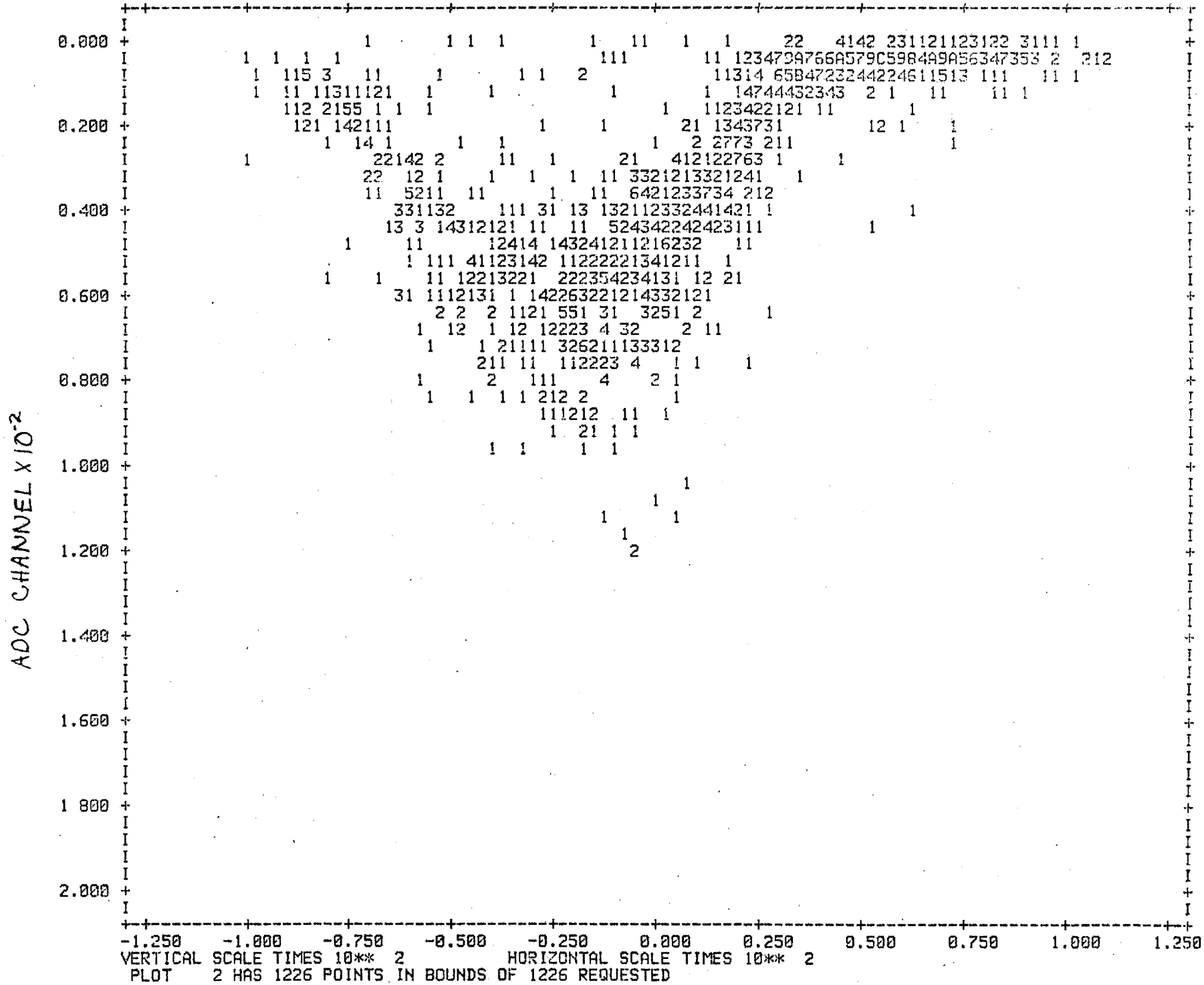

Fig. A2 PROJECTED TRACK ANGLE X 10^{-2} (mRAD)

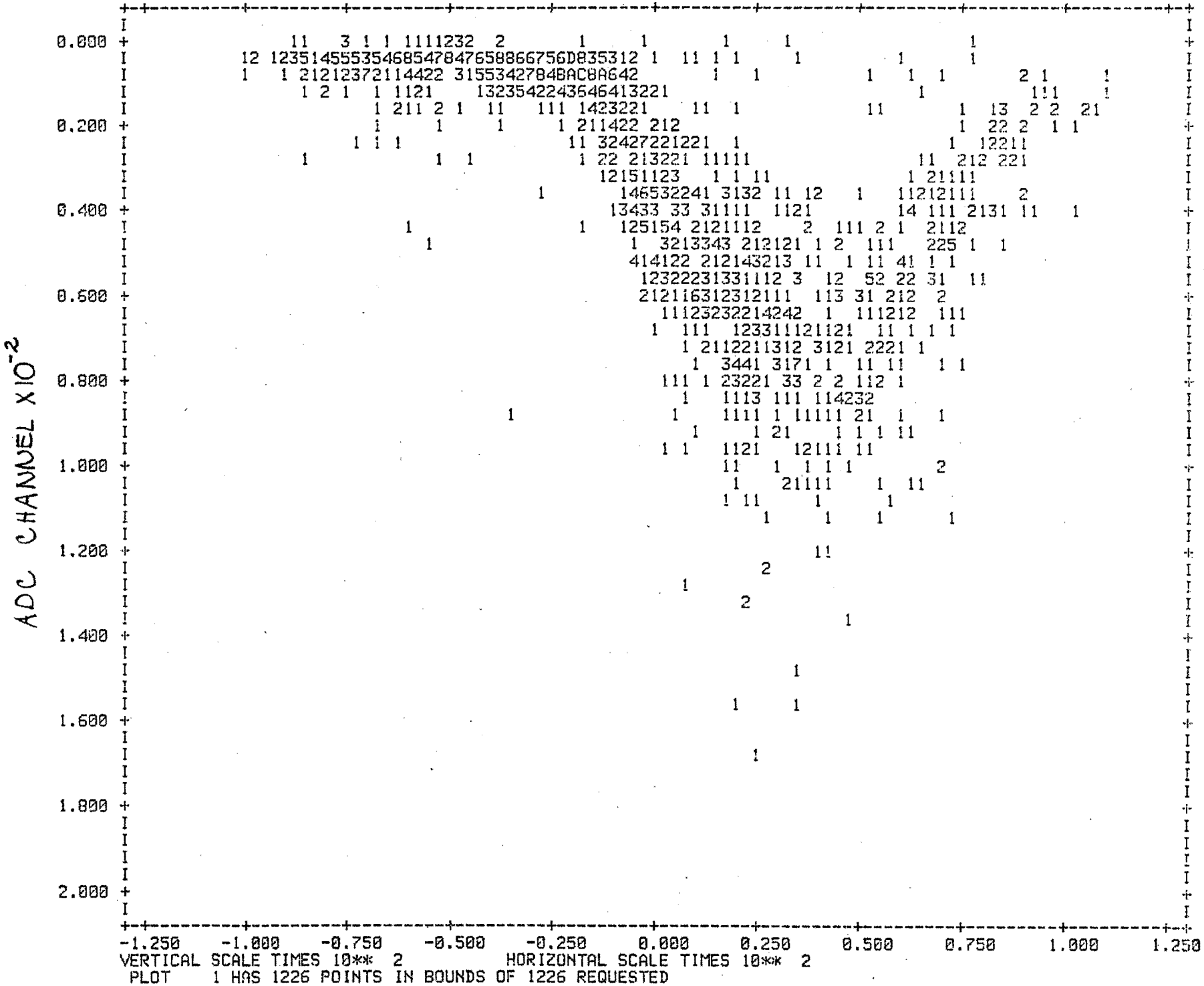

Fig. A3 PROJECTED TRACK ANGLE X 10^{-2} (mRAD)

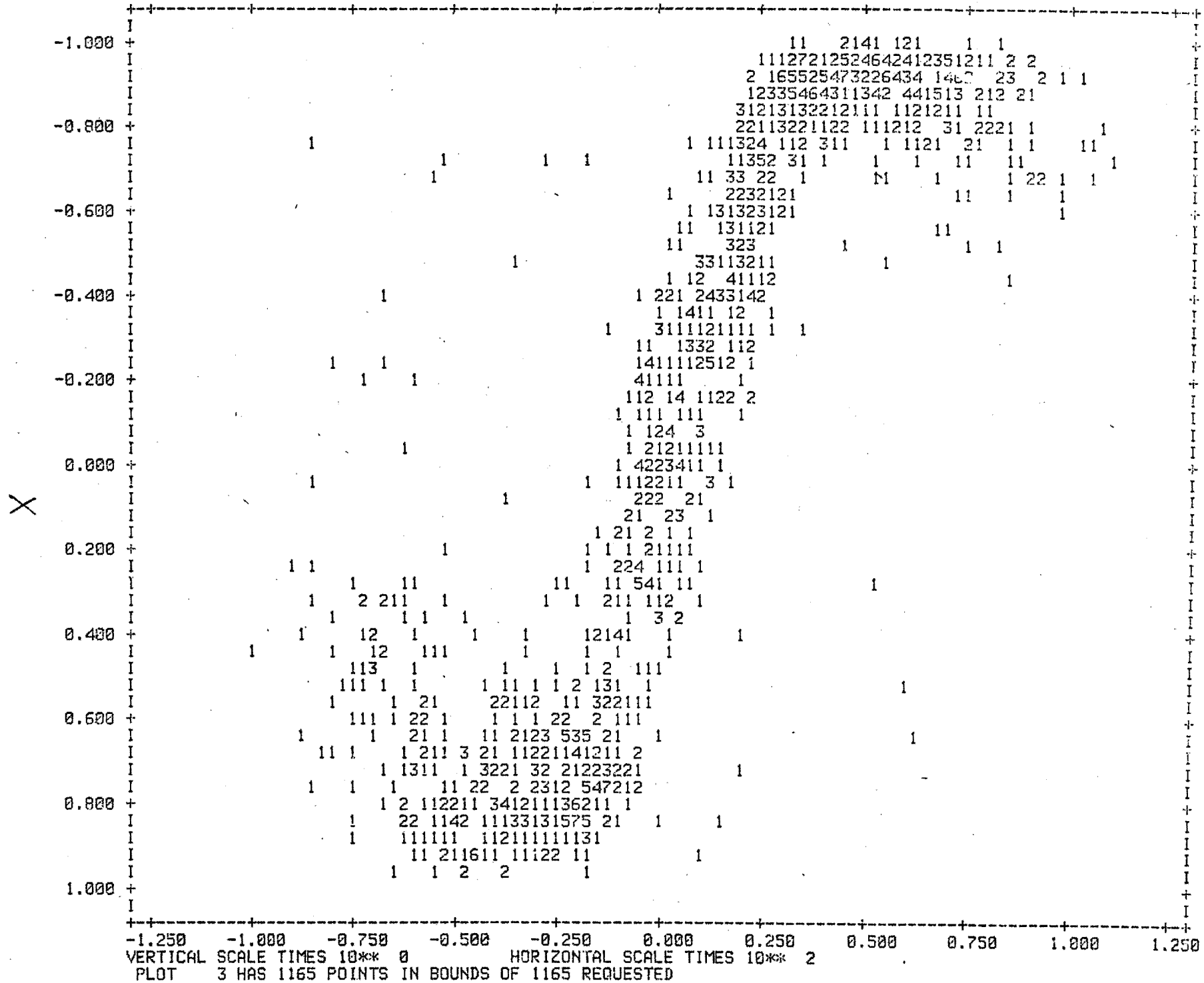

Fig. A4 PROJECTED TRACK ANGLE X 10^{-2} (m RAD)

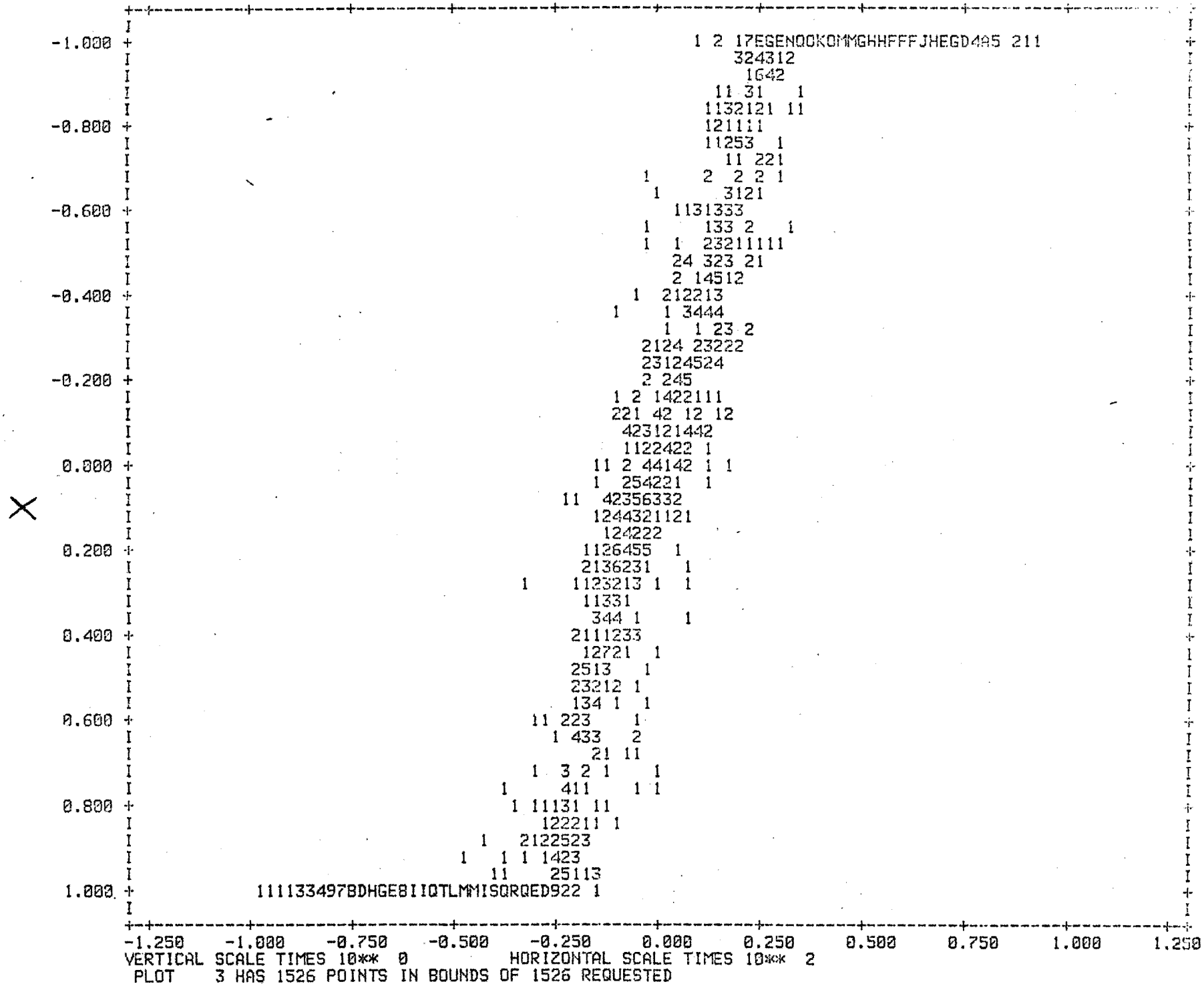

Fig. A5 PROJECTED TRACK ANGLE $\times 10^{-2}$ (m RAD)